EXPERIMENTAL AXIAL EVOLUTION OF THE WING-TIP VORTEX IN THE NEAR FIELD OF A NACA0012 AIRFOIL

C. del Pino, R. Fernandez-Prats, J.M. Lopez-Alonso, L. Parras, and R. Fernandez-Feria
ETSI Industriales, University of Málaga, 29071 Málaga, Spain

Abstract

In this experimental work we have undertaken a systematic visualization of the trailing vortex behind a NACA0012 airfoil at several distances near the wing tip for three angles of attack and two Reynolds numbers to characterize the structure of the vortex meandering phenomenon as well as its frequency, wavelength, and amplitude. The visualization technique allows us to characterize the downstream evolution of the vortex meandering up to sixteen chords. The results based on the amplitude versus the angle of attack show that there is no significant dependence on the Reynolds number from 0.5 till 6 chords. However, starting at 12 chords and up to 16 chords the variation of the vortex meandering amplitude depends slightly on the Reynolds number, so the amplitude is smaller as the Reynolds number is increased. In addition, the amplitude of the vortex meandering grows from the wing up to 12 chords, and then it remains approximately constant.

1. Introduction

Wing tip vortices (also called trailing vortices) are unstable tubes of circulating air which are left behind a wing as it generates lift, based on the Kelvin-Helmholtz theorem. Vortex meandering (or wandering) is a typical feature of wing-tip vortices that consists in a random fluctuation of its vortex centreline [1].

The precise knowledge of the dynamics, and the control, of trailing vortices in the wake behind aircrafts are relevant problems in civil or militar aviation, for these vortices strongly affect the frequencies of taking off and landing of aircrafts in an airport [2, 3, 4, 5]. The interaction of an aircraft wake vortex with a following plane is most likely near airport runways both because planes are likely to fly in close proximity when they are near the runway, and because the tip vortex circulation is maximal when a plane is taking off or landing [2]. To appreciate the severity of the interaction that occur when a plane encounters such wing tip, or trailing, vortices, the maximum tangential velocity around the Boeing 757 tip vortex in landing approach has been measured to be around 100 m/s, and greater than 10 m/s several meters from the centerline. A following plane travelling at a speed of say 60 m/s (typical for landing), which flies axially into the tip vortex generated by a B-757, therefore experiences an incident angle of attack of about 10 degrees above nominal on one wing surface and 10 degrees below nominal on the other. These huge changes in incident flow angle as the following plane enters the tip vortex can both stall the wing and generate large rolling moments that the aircraft ailerons cannot control. Since all this happens close to the ground, the most likely consequence is the crash of the plane, and many accidents of this type involving loss of life or serious injury have been reported in the past.

These problems have become even more important in recent years with the advent of the giant of the commercial aviation Airbus 380, which generates more persistent and more intense trailing vortices than smaller aircrafts. In order to avoid wake vortex encounters, safety separation distances have been set by the International Civil Aviation Organisation (ICAO). They take the form of a coarse matrix subdividing aircraft into light, medium, heavy, and now super heavy, classes, providing safe separation distances in the wake of each [6]. The separation distances range from two nautical miles (nm) for a heavy aircraft encountering the tip vortex of a small aircraft, to 9 nm for a small aircraft following the giant A-380. These very large commercial transports will be less attractive if larger traffic control separations cancel any advantage in terms of arriving seats per hour and per runaway. Any procedure to increase arrival frequencies with the same level of safety would be most welcome, and could save the construction of new runaways or entire airports. The financial implications of these landing separation requirements are enormous. It has been estimated that more than five millions euro could be saved annually at an airport the size of Franckfurt's if it were possible to land one additional aircraft per hour at each runway. Clearly, these financial implications alone justify research aimed to reducing the landing requirements necessitated by the wake vortex hazard.

Although the main technological motivation of this work has been the wake-vortex interaction when a plane flies through or near the tip vortex generated by a preceding plane, some other technological problems may benefit from the precise knowledge of the structure of tip vortices, such as the problem of reducing the lift induced drag originated by tip vortices, the optimization of the tip vortex interaction with rotor blades in helicopters and propellers, which cause rotor blade fatigue failure and excessive rotor blade noise, and the minimization of the hazard during aerial refuelling of a fighter aircraft by a tanker, among others [7].

There exists a very abundant literature, from the 1960s and even earlier, on the structure of trailing vortices in both a theoretical and experimental points of view (for more details, see [8]). One of the main difficulties of measuring the velocity field in a wing tip vortex is the meandering phenomenon, or random fluctuation of the vortex centerline [9]. This meandering is quite significant a few chords downstream a wing, but it is less pronounced within a chord of the trailing edge. A consequence of the meandering, also called wandering, phenomenon is that vortices measured by static measuring techniques appear to be more diffuse than in reality, so that a correction method is needed [10, 11].

In this work we have carried out experimental tests in order to visualize the trailing vortex behind a NACA0012 airfoil at several distances near the wing tip (0.5, 3, 4, 6, 12, 16 chords) for three angles of attack (6, 9 and 12 degrees) and two Reynolds numbers (23888 and 34192) to characterize the structure of the vortex meandering phenomenon as well as its frequency, wavelength, and amplitude. The technique is similar to that used by Roy and Leweke [12]. In the previous work with the same experimental set-up [13], it was proved that the Reynolds number has not a significant effect on the meandering amplitude in the near field (up to 4 chords). Thus, only two Reynolds numbers are tested in this study. However, the axial evolution of the vortex is deeply analysed in this study. For this reason, we explore larger downstream distances from the wing (up to sixteen chords).

2. Experimental set-up

The experiments were carried out in the same experimental set-up that is described in detail in [13]. Basically, a closed circuit, horizontal water tunnel facility with a working section of 0.5 x 0.5 m^2 cross-section and 5m long installed in the Laboratory of Aero-Hydrodynamics of Vehicles at the University of Málaga is used. This long test section is made of *Plexiglas* to allow for optical visualizations, as well as for PIV quantitative measurements of the velocity field [8], all along its five meters long. The range of velocities (V) tested are 20.4±0.4 cm/s and 29.2±0.4 cm/s, which are achieved through two *ABB* centrifugal pumps of 18.5kW each. The flow rate is measured through a turbine FLS flow meter (model Flowx3), located downstream of the pump, which was previously calibrated through LDA and PIV measurements of the axial velocity field at several cross-sections. Typically, the turbulence intensity is low, so the mean level is close to 3%. This is achieved by means of honey combs and nets included in the water-conditioned chamber.

To generate a single wing-tip vortex we use a NACA0012 symmetric airfoil with a chord c=100 mm, a length of 200 mm, vertically mounted on the upper surface of the first sector of the channel working section, and with the rounded tip approximately centred in the test section. The rotation of the wing into several positions is possible by means of a round window. Thus different angles of attack between the upstream flow and the wing are allowed. In addition, this window is provided with a connection between the system of controlled injection of dye and the wing, permitting flow visualizations in the wake behind the wing tip. The airfoil was machined in aluminium, and painted with a special black pigment to minimize corrosion by water.

For the visualization of the trailing vortex we used a green fluorescent dye (Rhodamin 6G) diluted in water. The dye is excited thanks to a laser of 40 mW (wavelength = 532nm). Consequently, the wing-tip vortex stands out from the rest of flow.

To record the vortex images we used a *Sony Handycam HDR-SR5* video-camera with a resolution of 1 Mpixel, 40 Gb of internal memory, and a maximum shutter speed of 1/25s (see Figure 1). The speed of 25 frames per second was found to be enough to characterize the meandering phenomena, whose main frequency was always well below 1Hz (see next section). An optical window is mounted to neglect the out of focus images.

Figure 1: Photograph showing the camera and the optical window used to obtain the images.

The main features of the wing-tip vortex sought from the image processing are the frequency and wavelength of the fluctuations (meandering), the distribution of the vortex centre positions, the angle of the main direction of these fluctuations, their amplitude, and the spatial structure of the principal or most energetic oscillation modes. However, more information and new details are shown below to better understand the features of the experimental set-up:

In the experimental set-up we should take into account that the views with the camera must always be on the opposite side of the laser. This setup is then accurate enough, since the camera and the laser located on the same side of the tunnel, imply that the visualizations are of poor quality. Therefore, a wrong set up adds more difficulties on the image processing, due to the fact that the pigments (Rhodamine 6G and fluorescein) are less excited as they are not faced with the scattering of the laser.

The dye injection system is regulated in order to obtain an uniform picture behind the wing. Thus, the amount of dye must be the same for each experimental run. To make a right image processing, the vortex wandering must be also visualized in the each frame. To that end, the intensity of the vortex must be bigger than the laser one. On the other hand, the flow rate of the dye injection has to be small enough, so that its velocity has not influence on the vortex structure.

We must use enough Rhodamine 6G to obtain images of good quality in each test. This pigment tends to form clots in the nets, leading to turbulence. The net must be cleaned frequently.

It is important to choose the right size of a target matrix depending on the vortex meandering amplitude. For distances near the wing a 90x90mm2 target is used, as the 180x180mm2 is needed for distances bigger than 12 chords (see Figure 2). The small target has 36x36 white dots separated 2.5 mm, as the big one has 18x18 white dots separated 10 mm.

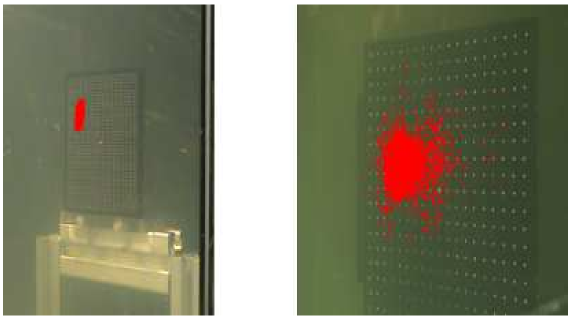

Figure 2: The centres of the vortex computed are superimposed with red dots in the small (left) and the big (right) targets.

It is essential to ensure that the centres of the vortex are within target, since it appears that the calibration and subsequent transformation to process the frames are only valid within the region of the input points.

New additions of this work related to the Statistical analysis of the vortex centre position are also described as follows: the computing programs and the image processing used a *Warping algorithm* instead of *Mapping algorithm*, largely due to the computation time requirements. the reduction in the computing time is based on how many pixels are transformed from the recorded to the real plane. In the case of the Mapping algorithm, we should apply the transformation in all the images, since the Warping algorithm is only used for the centres of the vortex. The parameters calculated by both techniques in this investigation do not change, so we guarantee the results of the previous work [13], see next section.

Note that an incorrect choice of the input points in the calibration process generates big errors in the calculations, so the vortex cores outside the transformation area of the target are wrong. As it is already explained in [13], the image of the target is transformed into a square by means of a bilinear transformation of a number of points. Since this transformation contains 12 unknown coefficients, we select at least 6 points of the target (x_i,y_i), and transform them into the calibrated, or transformed, points (X_i,Y_i). These six points are selected on the total of the calibration target. Figure 3 (a) shows the target in the (x,y) and figures (b) and (c) the (X,Y)-planes, when the transformation is applied in the whole target (b, desired) or only in the second quadrant (c, bad processed).

The cases studied in this work are summarized in the table 1.

Q(l/s)	U (cm/s)	Re	T(ºC)
51±2	20.4±0.4	23888±468	27.5±2
73±2	29.2±0.4	34192±468	27.5±2

Table 1: Flow rate Q, mean velocity V=Q/A, where A is the area of the test section of the tunnel, and Reynolds number Re=Vc/ν, where c is the wing chord and ν the kinematic viscosity of water. The errors in the Reynolds number take into account not only the fluctuations in the flow rate, but also those associated to the measured temperature through the kinematic viscosity, which is computed using an experimental relation given in White [14].

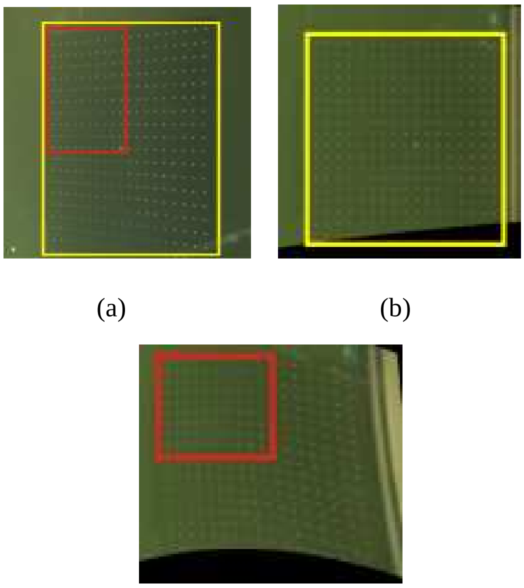

(a) (b)

(c)

Figure 3: Images of the big calibration target before [(a), (x,y)-plane, left] and after [(b)-(c), (X,Y)-plane, right] the transformation. The correct transformation corresponds to the plot (b). A significant deformation is observed in the picture (c) outside the red box.

3. Quantifying magnitudes from views

3.1 Statistical analysis of the vortex centre position

The movement of some flows are complex and it is really a challenge its theoretical study, so different techniques have arised to quantify the visualizations. With these techniques we are able to visualize the majority of the flows. Thus, these techniques are a fundamental tool for doing research and analyzing new phenomena. It is worth to mention that these techniques do not introduce elements that disrupt the flow because they use the information obtained from the visualizations. This section will describe the different techniques used to quantify the phenomenon of vortex meandering. To obtain reliable data from the visualizations we have been developing, optimizing and correcting algorithms that fit within what is called computer vision, from which it derives the digital image processing. This can be defined as the set of techniques and algorithms applied to digital images with different objectives. There are two main groups for the different processing techniques:

A) Spatial techniques: Geometrical transformations, Spatial Filters, Arimtethic operations, Unsharp masking.
B) Spectral techniques: Convolution, correlation, maximun entrophy method.

The computational vision has been one of the disciplines that has experienced a spectacular growth in the recent years, largely due to many applications and implications that may result in other Sciences, so it is a valued resource for research tasks.

The spatial calibration was the first algorithm that has been applied to the images recorded. For a given set of parameters, we estimate the distribution of the positions of their centres at different time steps. Although the philosophy is the same, the method developed in this work is slightly different to the one used in [13]. Basically, the position of the vortex core is computed by means of a threshold segmentation technique applied to the original images. Then, the transformation from the (x,y) to the (X,Y) plane is used. This is the main difference: we do not need to transform all the pixels of each frame, so only the transformation is applied to the centre of gravity. To compare the two methods, we choose the case of Reynolds number 34192, angle of attack of 12 degrees and the axial position is z/c=16. The results are depicted in Figure 4 and one can observes that there is no difference between the two methods.

The operation is repeated for every image captured by the video-camera in a run (about 16,500 frames) for a given flow rate, angle of attack, and distance to the wing, so that a statistical treatment of the transverse position of the vortex centre can be made. To characterize the distribution of the transverse position of the vortex centre we compute the eigenvalues a_M^2 and a_m^2 of the covariance matrix of the vectors x_c and y_c. For $a_M^2 > a_m^2$, the two corresponding eigenvectors $\mathbf{v}_M$ and $\mathbf{v}_m$ are the directions in which the statistical dispersion is maximal and minimal, respectively, the eigenvalues being the corresponding variances in both directions. a_M and a_m can be considered as dispersion radii in the $\mathbf{v}_M$ and $\mathbf{v}_m$ directions (see Figure 5). Finally, an angle β can be defined between the horizontal direction and the direction of the major axis $\mathbf{v}_M$ of the vortex position distribution. We have corroborated that the error in the computations with 16,500 frames is about one hundredth of a millimeter in the case of the dispersion radii (a_M, a_m) and 1 degree in the case of the angle β.

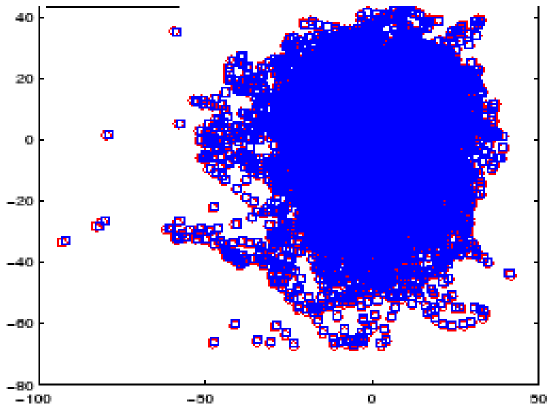

Figure 4: Distributions of the vortex centre positions for Re=34192, α=12º, and z/c=16. Coordinates are centred on the mean position. (x,y) plane dimensions are given in mm. Each blue square represents the centre position (x_c,y_c) in one visualization frame with the method of [13]. The red circles correspond to the method developed in this work.

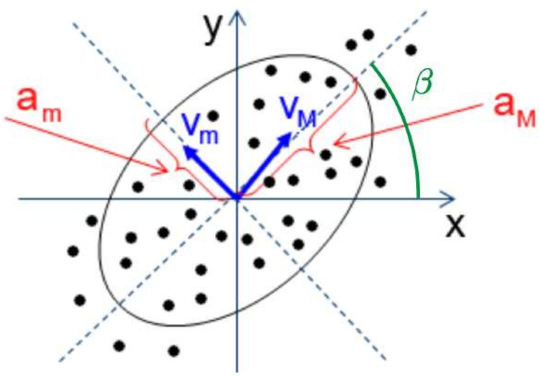

Figure 5: Sketch of the processed data after analyzing the distribution of the vortex centres.

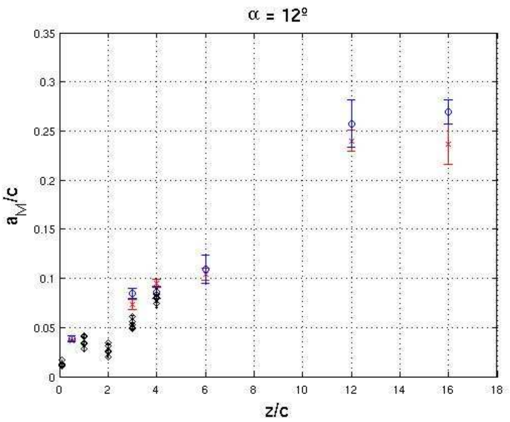

(a)

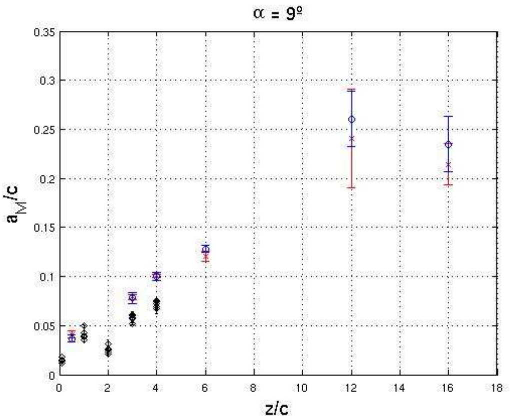

(b)

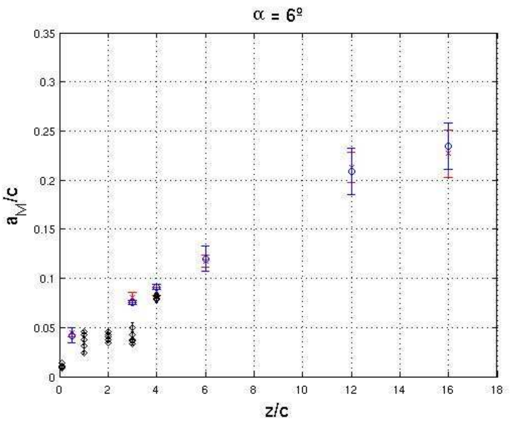

(c)

Figure 6: Axial evolution of the non dimensional radii a_M/c for two Reynolds numbers (23888, blue and 34192, red), and different angles of attack [α=12º (a), 9º (b) and 6º (c)]. The black points represent the data computed in [13].

Figures 6 shows the downstream evolution of the mean statistical properties of the vortex; i.e., a_M/c plotted against z/c for three angles of attack and the two Reynolds numbers considered in this work. These figures show that the influence of the Reynolds number on these mean quantities is quite small, except for the further locations (z/c bigger than 12). A slight reduction in the magnitude is observed as the Reynolds number is higher. For α=12º and 9º it is also clear that the amplitude of the vortex, characterized by the eigenvalues a_M^2 grows linearly up to z/c=12. After this position, the vortex meandering remains constant. In addition, the rollup process of the vortex sheet created by the lift of the wing develops in a region between the wing tip and two-three chords downstream, approximately (see [13]), until the vortex is formed. Then, the amplitude is still growing linearly up to z/c=12. For the smallest angle of attack considered, α= 6º, the region of vortex formation extends further downstream, so there is no significant saturation of the amplitude.

On the other hand, Figure 7 shows the downstream evolution of the mean statistical properties of the vortex; i.e., a_m/c plotted against z/c for the angles of attack given and the two Reynolds numbers computed. Obviously, the values of a_m/c are lower than a_M/c, except for the locations z/c bigger than 12, where both magnitudes are of the same order. These figures also show that the influence of the Reynolds number on these mean quantities (a_m/c) is bigger than in the previous magnitude (a_M/c). For all the angles of attack α the amplitude of the vortex, the eigenvalues a_m^2 also grows linearly up to z/c=12.

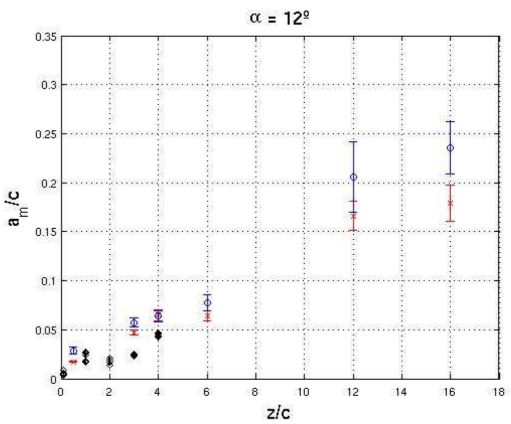

(a)

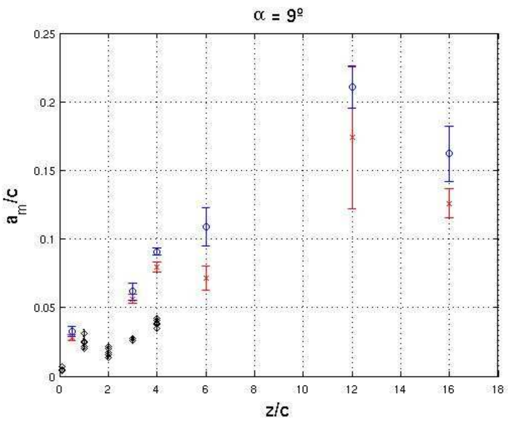

(b)

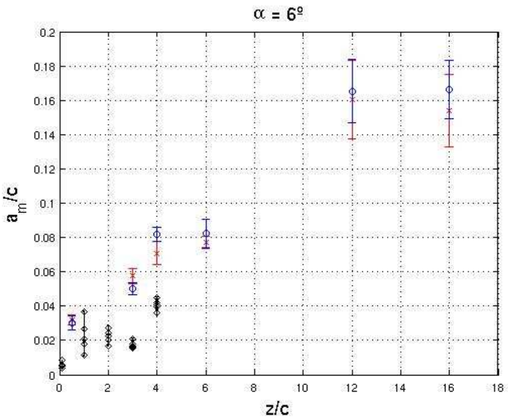

(c)

Figure 7: Axial evolution of the non dimensional radii a_m/c for two Reynolds numbers (23888, blue and 34192, red), and different angles of attack [α=12º (a), 9º (b) and 6º (c)]. The black points represent the data computed in [13].

The angle β (Figure 8), however, shows that the region of vortex formation extends in fact up to z/c=12 for two angles of attack α= 12º and 6º, with marked fluctuations in β up to this axial location z/c=12. Downstream this value, the angle β does not depend on the Reynolds number, so the downstream asymptote has been reached at z/c=16, and its value is close to 70º. Big fluctuations are observed in the case of α= 9º, although the mean angle is approximately of the same order.

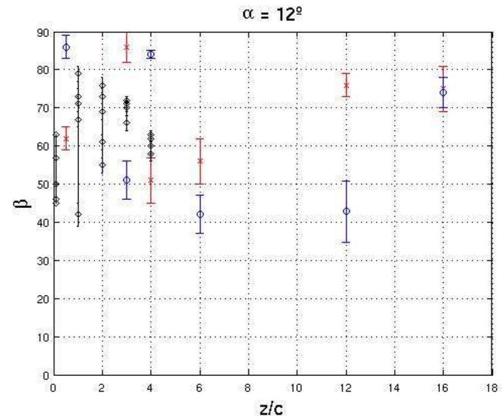

(a)

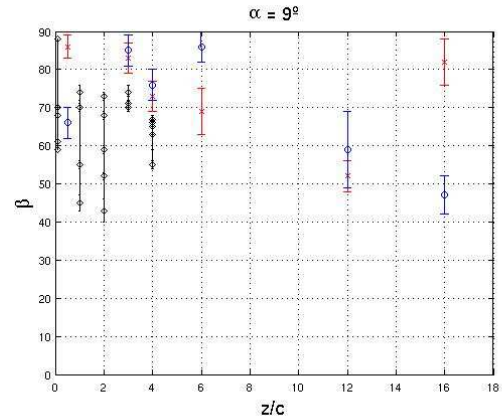

(b)

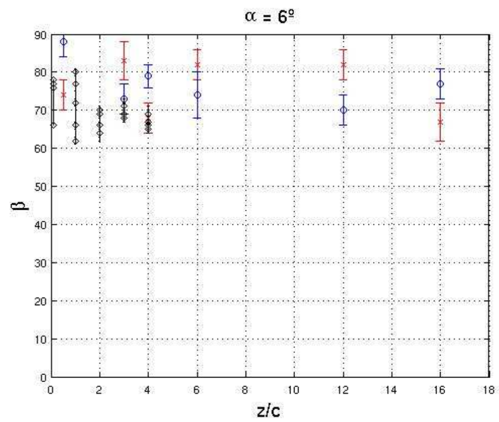

(c)

Figure 8: Axial evolution of the angle β for two Reynolds numbers (23888, blue and 34192, red), and different angles of attack [α=12º (a), 9º (b) and 6º (c)]. The black points represent the data computed in [13].

In summary, the amplitude and the angle of the vortex fluctuations characterized from images captured at several axial locations downstream the wing show that a vortex is formed between the wing tip and 2 or 3 chords downstream, depending on the angle of attack [13]. Downstream this region, the values of the radii grow linearly up to z/c=12, and then they reach asymptotic values downstream, and its angle remains approximately constant (70º).

3.2 Vortex perturbation structure

The previous section was concerned about describing the process to compute the vortex core and its connection with the physical parameters and the axial evolution. This section will focus on investigating the nature of the disturbances of the vortex. First, we examine the spatial structure of these disturbances described by identifying the most energetic modes. Then and focusing on these most energetic modes, we perform a spectral analysis mode of the perturbations, so we can characterize the frequency and wavelength of the meandering of the vortex. An efficient way to extract a set of modes characterizing the perturbation of a given base flow is to perform a singular value decomposition, or Proper Orthogonal Decomposition (POD), which has been extensively used to characterize turbulent flows [12, 15]. This method is carefully explained in [13]. In this work we take 16,500 images instead of 13,000 images.

To illustrate the POD method, Figure 9 shows the results for the case α=12º, Re=23888 and z/c=3. The (x,y)-plane dimensions are given in pixels. One can observe that for all the tests carried out in this work, the most amplified picture after applying the POD method is almost axisymmetric shape that corresponds to the base flow (a). In addition, the following most energetic modes are related to the eigenvectors $\mathbf{v}_M$ and $\mathbf{v}_m$ [(b) and (c)], so this disturbance has an azimuthal wave number equals to 1. The angle βcould be also be estimated thanks to the POD method. Finally, another (less energetic modes) are depicted in (d) and (e). These last modes correspond to elliptical deformations of the vortex core.

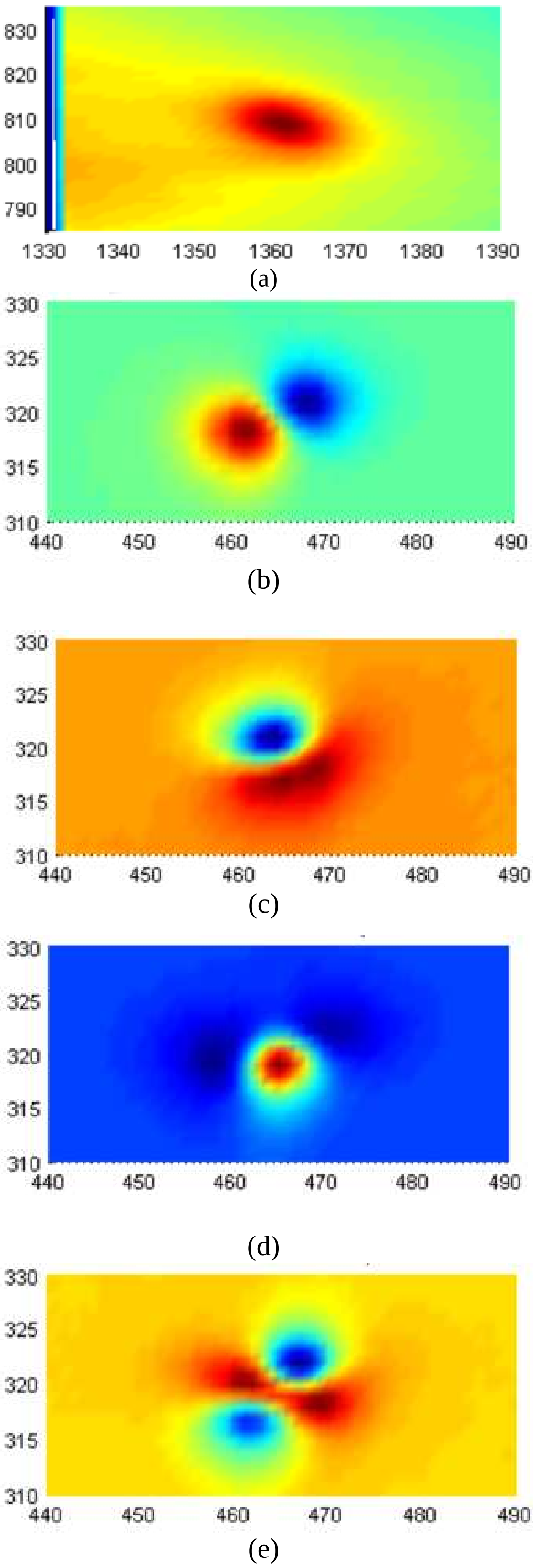

Figure 9: POD pictures results for the case α=12º, Re=23888 and z/c=3. The fifth energetic modes are depicted from (a) to (e), as the energy of the perturbations decreased.

On the other hand, one is able to obtain the frequencies after analyzing the POD images by means of the FFT method. The non dimensional wavelengths, U/(f c), are depicted in Figure 10 for the two Reynolds numbers considered, and for the three values of the angle of attack considered. The main conclusion is that, although in same particular cases big oscillations are observed, the tendency or mean value in all the cases is near 10^2. This value is about 1-2 orders of magnitude bigger than the results reported in another investigations [10, 12, 16]. For this reason, more experimental effort is needed to better understand this fact. How the level of turbulence affects the results is one of the questions that must be clarified.

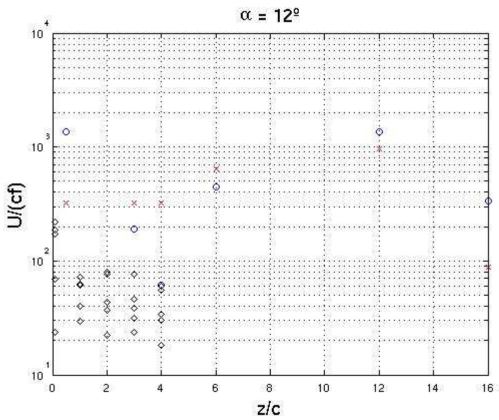

(a)

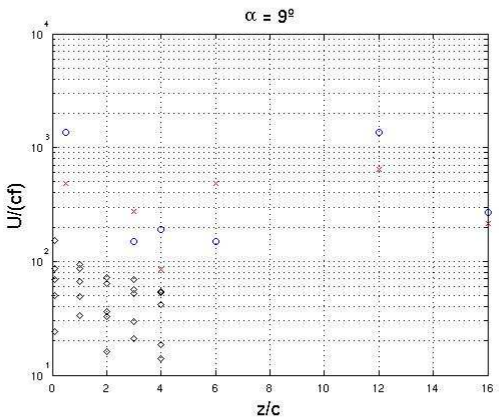

(b)

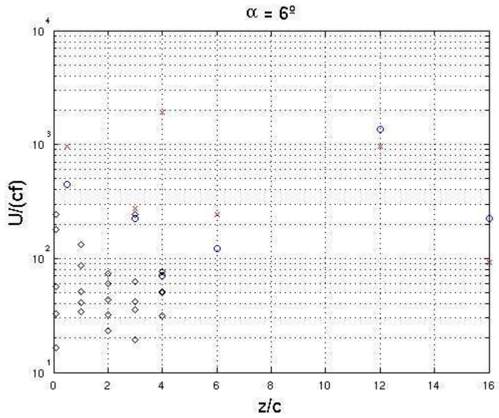

(c)

Figure 10: Evolution with z/c of the main non-dimensional wavelength U/(f_p c), for the two Reynolds numbers considered (), and for the three values of the angle of attack considered, as indicated in (a) - (c).

4. Conclusions.

We have characterized the meandering phenomenon of a wing-tip vortex in the near field behind a NACA 0012 airfoil by quantitative analysis of the images taken at different cross sections (z/c =0.5, 3, 4, 6, 12 and 16) downstream of the wing trailing edge. We have processed 16,500 images taken at a rate of 25 frames per second at each downstream location, for three different angles of attack (6º, 9º, and 12º), and for two different Reynolds numbers (23888 and 34192). In particular, we have characterized the downstream distribution of the vortex centre, and the amplitude and angle of their wandering oscillations. We find that after the vortex formation the values of the radii grow linearly up to z/c=12. The results show that after this axial position, the vortex meandering does not increase its size. We have also characterized the structure of the wandering phenomenon by means of a POD analysis of the images, finding that the most energetic mode of the perturbations of the original axisymmetric vortex has an azimuthal wavenumber n=1, in agreement with previous results [12, 13].

One of the main conclusions of the present work is that the main frequency of this most energetic, or dominant, perturbation mode of the vortex coincides with the main frequency obtained from the analysis of the distribution of the vortex centre positions and, therefore, characterizes the vortex meandering frequency. But the values obtained in the present work, of the order of 10^{-2} -10^{-1} Hz, are almost one-two orders of magnitude smaller than in previously related works [10, 12, 16]

References.

[1] L. J. Clancy, *Aerodynamics*, Pitman Publishing Limited, London, 1975.

[2] Th. Gertz, F. Holzapfel, W. Bryant, F. Kopp, M. Frech, A. Ta□erner, and G. Winckelmans. Research towards a wake-vortex advisory system for optimal aircraft spacing. Comptes Rendus Physique, 6:501–523, 2005.

[3] Th. Gertz, F. Holzapfel, and D. Darracq. Commercial aircraft wake vortices. Prog. Aero. Sci., 38:181–208, 2002.

[4] P. Spalart. Airplane trailing vortices. Ann. Rev. Fluid Mech., 30:107–138, 1998.

[5] S. E. Widnall. The structure and dynamics of vortex filaments. Ann. Rev. Fluid Mech., 7:141–165, 1975.

[6] M. Kingsley-Jones. Airbus confident on A380 wake ruling. Air Transport, pages http://www.flightglobal.com /articles/2006/06/20/207265/airbus–confident–on–a380, 2006.

[7] S. I. Green. Wing tip vortices. In S. I. Green, editor, Fluid vortices, pages 317–372. Kluwer, 1995.

[8] C. del Pino, L. Parras, M. Felli and R. Fernandez Feria. Structure of trailing vortices: comparison between PIV measurements and theoretical models, *submitted* to Physics of Fluids.

[9] C. del Pino, L. Parras, M. Felli and R. Fernandez Feria. PIV measurements of the structure of wing-tip trailing vortices and their comparison with theoretical models, 15th Int Symp on Applications of Laser Techniques to Fluid Mechanics Lisbon, Portugal, 05-08 July, 2010.

[10] W. J. Devenport, M. C. Rife, S. I. Liapis, and G. J. Follin. The structure and development of a wing-tip vortex. J. Fluid Mech., 312:67–106, 1996.

[11] S. K. Iungo, P. Skiner, and G. Buresti. Correction of wandering smoothing e□ects on static measurements of a wing-tip vortex. Exp. Fluids, 46:435–452, 2009.

[12] C. Roy and T. Leweke. Experiments on vortex meandering. Technical Report TR 1.1.1-4 STREP project no. AST4-CT-2005-012238, Fundamental research on aircraft wake phenomena (FAR-Wake), CNRS-IRPHE, 2008.

[13] C. Del Pino, J.M. Lopez-Alonso, L. Parras, and R. Fernandez Feria. Dynamics of the wing-tip vortex in the near field of a NACA0012 airfoil. Proceeding paper, European Air and Space Conference. Manchester 2009, DISBN 1857682084, *submitted* to Journal of Aircraft.

[14] F.M. White. *Fluid Mechanics*. McGraw-Hill, New York, 2005 (Fifth ed.).

[15] G. Berkooz, P. Holmes, and Lumley J. L. The proper orthogonal decomposition in the analysis of turbulent flows. *Annu. Rev. Fluid Mech.*, 25:539–575, 1993.

[16] S. C. C. Bailey and S. Tavoularis. Measurements of the velocity field of a wing-tip vortex, wandering in grid turbulence. *J. Fluid Mech.*, 601:281–315, 2008.